Reply to the comments of anonymous Referee #1 to Li et al., "Atmospheric column CO_2 measurement from a new automatic ground-based sun photometer in Beijing from 2010 to 2012", Atmos. Meas. Tech. Discuss., 5, 8313-8341, 2012

The authors thank very much the constructive suggestions from the anonymous referee. We decide to make substantial corrections to the manuscript. Details are described below:

Question 1

The DAI index seems to represent the slant column CO2 amount. At no point in the manuscript do the authors mention that they have taken into account the fact that since their measurement is direct sun, the CO2 column that needs to be computed is the vertical column. This can be done either through a radiative transfer model, or more simply, an off-line airmass calculation given the known location and time of the measurements. Until this is done, the CO2 presented here is driven mostly by airmass dependence. This particular issue therefore affects all subsequent discussion in the manuscript with respect to diurnal, seasonal and model comparisons.

Reply: We agree with the referee's opinion on the airmass effect. We refine the definition of DAI with consideration of slant path correction (see below):

Based on Beer-Lambert law, the direct sun measurement of the CO_2 instrument can be expressed by:

$$V = V_0(\frac{d_0}{d})^2 \exp(-m\tau) \qquad (2)$$

Where V is the signal of the instrument at surface of the Earth; V_0 denotes the instrument signal at the top of atmosphere, i.e. the absolute calibration coefficient; $(d_0/d)^2$ is the Sun-Earth distance correction factor; m is the airmass, and τ is the atmospheric total optical depth (TOD) which can be separated into three parts: the aerosol optical depth (AOD) τ_{aer}, the Rayleigh optical depth (ROD) τ_{Ray} and the gases optical depth (GOD) τ_{gas}:

$$\tau = \tau_{aer} + \tau_{Ray} + \tau_{gas} \qquad (3)$$

By noting the subscript *a* and *b* for absorption and base channels respectively, we can derive channel signal ratio following the difference absorption principle:

$$\ln\frac{V_b}{V_a} = \ln\frac{V_{0,b}}{V_{0,a}} + m(\tau_a - \tau_b) \qquad (4)$$

By jointing eq. (3) and (4), we can define the DAI index, related to the optical depth of CO_2 as:

$$\begin{aligned} \mathrm{DAI} &= \tau_{gas,a} - \tau_{gas,b} = (\tau_a - \tau_b) - (\tau_{aer,a} - \tau_{aer,b}) - (\tau_{Ray,a} - \tau_{Ray,b}) \\ &= \frac{1}{m}\left(\ln\frac{V_b}{V_a} - \ln\frac{V_{0,b}}{V_{0,a}}\right) - \tau_{aer,b}\left[\left(\frac{\lambda_a}{\lambda_b}\right)^{-\alpha} - 1\right] \end{aligned} \qquad (5)$$

In this equation, we consider the difference in GOD coming only from CO_2 and ignore other gases contribution to the optical depth at the selected channels. Differences of Rayleigh optical depth at two channels are small enough and assumed to be ignored. The uncertainty caused by these assumptions will be discussed in the error analysis part of the paper, while we deduce the aerosol influence in term of AOD at base channel and Angstrom coefficient α in Eq. (5). Moreover, the airmass *m* can be computed from solar zenith angle (Kasten, 1989). The absolute calibration coefficient $V_{0,b}$ and $V_{0,a}$ are not calibrated in this study, but their ratios can be directly calculated following:

$$\frac{V_{0,b}}{V_{0,a}} = \frac{\int E_s(\lambda)R_b(\lambda)d\lambda}{\int E_s(\lambda)R_a(\lambda)d\lambda} \qquad (6)$$

Where R_b and R_a are filter transmission profiles of two channels, and E_s the extraterrestrial solar irradiance which can be obtained, for example from ASTM-STD-2000 (http://rredc.nrel.gov/solar/spectra/am0/). Advantages for the use of DAI as the CO_2 column content index include not only avoiding absolute calibration of V_0, but also resisting the instrument changes thanks to the "ratio format" of the measurements and calibration coefficients as illustrated in Eq. (5) and (6).

According to the new treatment of the DAI index, we re-plotted the Fig. 7 and Fig. 8 as shown below. From these figures, the seasonal and yearly behaviors of the observed CO_2 DAI show similar properties compared with our previous manuscript. This is explained by the fact that the airmass correction affects firstly the daily behavior of the DAI instead of the seasonal and yearly behaviors, considering the airmass varies greatly in the day but not in the scale of daily average.

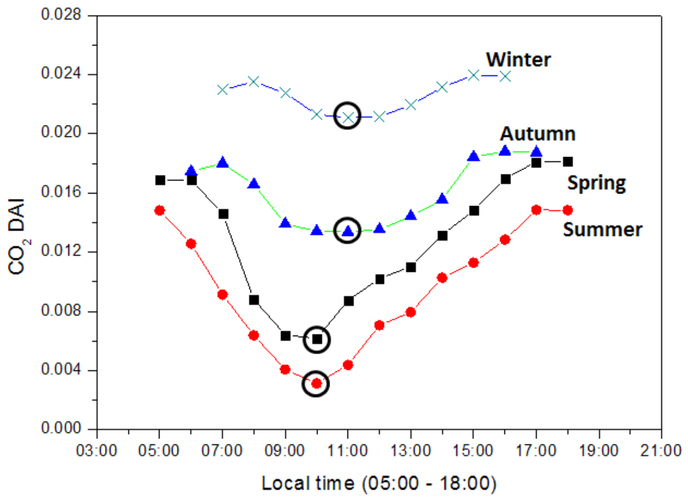

Fig. 7. Daily averaged CO_2 DAI at different seasons in Beijing during 2010-2012.

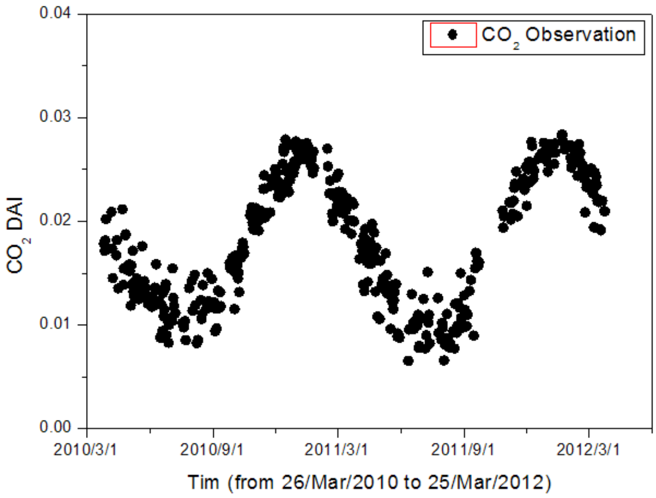

Fig. 8. The seasonal variation of CO2 DAI in two years from 2010 to 2012, IRSA site, Beijing.

Question 2

So, based on issue 1) above, the comparison with CarbonTacker invariably is comparing the dry air mode fraction (xCO2) against a slant column (figure 10). The correlation is largely driven by the seasonal cycle in the airmass rather than changes in the XCO2.

Reply: According to reply of Question 1, we reproduced the vertical corrected CO_2 DAI, and compared with CarbonTacker results as shown below in Fig.10. We also made a small improvement in the figure to show the ±1 ppm threshold boundary lines, instead of previous dash line, considering that 1ppm is the general expectation for ground-based CO_2 measurements. It is noted that there are DAI points beyond this threshold, which is discussed in the error analysis part. Also, the CO_2 sunphotometer measurements are expected to be improved for the calibration and data processing aspects in the next studies.

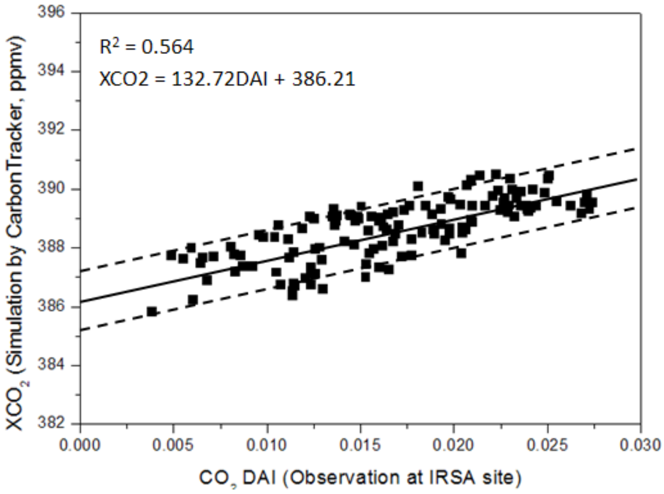

Fig. 10. The correlation plot of daily averaged CO_2 amounts between CarbonTracker model and the observation at IRSA site for the same period (March to December in 2010). The solid line denotes the linear fitting of the observed and modeled CO_2 while dash lines showing ±1 ppm threshold.

Question 3

Since this is a measurement paper, there must be a full description of the errors. This not addressed at all in this paper.

Reply：We added error estimation following new treatment of DAI definition (please see below).

The error estimation of DAI are discussed following uncertainty resources on:

(i) Aerosol

In Eq. (5), we developped the AOD correction item, and in this study the needed aerosol parameters can be obtained from the aside CIMEL CE318 sunphotometer. Assuming the errors in $\tau_{aer,b}$ is 0.02 (Holben et al., 1998) and employing the multi-year averaged α (=1.08) observed in Beijing by the Aerosol Robotic Network (AERONET) (Holben et al., 1998), we estimated a typical error of about 1.4×10^{-4} on DAI caused by uncertainty on aerosol measurements.

(ii) Rayleigh scattering

Rayleigh scattering optical depth in the 1560-1580 nm region is very small since ROD is proportional to λ^{-4}. Uncertainties caused by Rayleigh optical depth are in the order of 10^{-7} on DAI and can be safely neglected in this study.

(iii) Other gas absorption

Absorption of other gases such as water vapor, ozone in these channels are very small and can be neglected.

(iv) Instrumental issues

The DAI uncertainties can also come from instrumental issues, like sun-tracking error, measuring time precision, and filter response profile degradation. However, the influence of these factors are expected to be small in this study, considering the difference absorption principle used for DAI. We estimate an uncertainty of about 0.5% on DAI from instrumental issues.

(v) Cloud contamination

The current cloud screening procedure may miss some optical thin cirrus as discussed in the cloud screening part. In these cases, the DAI might be overestimated. Error caused by this uncertainty is difficult to be estimated but according to CIMEL aerosol sunphotometer experience (Smirnov et al., 2000), numbers of these cases are few and can be reduced by improving the cloud screening algorithm. Following above discussion, the total uncertainty is thus estimated to be about 1.2% assuming a typical DAI of 0.02.

Question 4

The authors use MODTRAN to compare a spectrum with the filter curves (figure 5). Why not produce a spectrum from MODTRAN at the effective resolution of the filters? By inspection the filter widths are about 4 nm (or around 16cm-1). In doing so this would be very instructive; this would show how the filters are sampling the CO2 1.6 micron band, how independent the base filter is, and more importantly, potentially provide a forward model that could be used in the analysis.

Reply: This is a very good suggestion. We re-produced the spectrum following the suggestion but found that there were some repetition by comparing with Fig.5 plus Fig. 6. In Figure 6 (a), the spectrum has been sampled to the effective resolution of the filter width interval, and the curve for CO_2 shows already, to a certain degree, how the filters are sampling the CO_2 spectrum. Therefore, we decide to keep the original Fig. 5 and 6 and improve the related statements in the text.

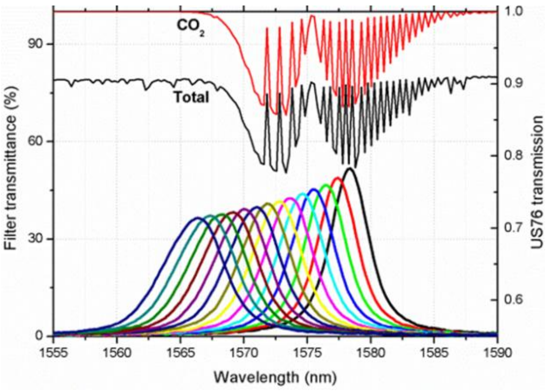

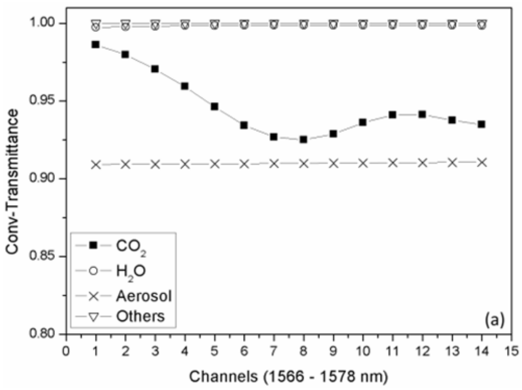

Fig. 5. The transmittance curves of CO_2 and the total atmosphere (right axis), calculated by Modtran with resolution of 4.0 nm, using US Standard Atmosphere of 1976. The 14 filter transmittance curves (centered from 1566 to 1578 nm of ASTSR) are displayed following left axis.

Fig. 6. (a) Convoluted transmittances of atmospheric constituents (with the transmittance of 14 filters of ASTSR). The transmittance of water vapor and other gases are very close to 1.00, causing little attenuation to the solar irradiance.

Question 5

The use of English throughout the manuscript needs significant improvement. There are too many sections that need a complete rewrite that makes it untenable for any referee to attempt correction.

Reply 5

Following the referee’s suggestion, we improved the English writing carefully throughout the manuscript.